

Randomly rough rectangular-groove surfaces with predetermined backscatter intensities

N.C. Bruce

Centro de Ciencias Aplicadas y Desarrollo Tecnológico, Universidad Nacional Autónoma de México, Circuito Exterior, Cd. Universitaria, Apartado Postal 70-186, México, D.F. 04510, México, e-mail: bruce@aleph.cinstrum.unam.mx

Recibido el 2 de febrero de 2006; aceptado el 18 de abril de 2006

The backscattered intensity of the scattered light in rectangular-grooved surfaces is used as a design parameter for randomly rough surfaces. A modified Kirchhoff method and the integral equation method are used to calculate the scattered light distribution for these designed surfaces. The results of the two calculation methods are found to show good agreement, with the Kirchhoff method slightly overestimating the double scattered intensity, perhaps due to the limitations of the geometrical shadow functions used in this method. These results show that the backscattered intensity can be controlled in this type of surface.

Keywords: Rough surfaces; scattering; Kirchhoff approximation.

Se utiliza la intensidad de la retrodispersión de la luz esparcida en una superficie con surcos de forma rectangular como parámetro de diseño de la superficie. El método de Kirchhoff modificado y el método de la ecuación integral son empleados para calcular la distribución de la luz reflejada de la superficie. Se encuentra que los resultados de los dos métodos están de acuerdo aunque el método de Kirchhoff sobre estima el esparcimiento doble, probablemente debido a las aproximaciones requeridas para las funciones de sombra geométrica utilizada. Los resultados presentados muestran que se puede controlar la intensidad en retrodispersión para este tipo de superficies.

Descriptores: Superficies rugosas, esparcimiento; aproximación de Kirchhoff.

PACS: 42.25.Fx; 42.25.Mj

1. Introduction

There has been a great deal of interest in recent years in the scattering of light from rough surfaces. In particular, light scattering from sea surfaces, and from Gaussian and fractal rough surfaces has been investigated both theoretically and experimentally. However, surfaces with a rectangular surface structure shape have not attracted as much attention. Jakeman and Hoenders [1] studied the statistics of the light scattered by a telegraph-wave surface of rectangular grooves distributed with a Poisson distribution of zero crossings. In this case, the grooves were the same depth but with variable width and separation. Similarly Depine and Skigin [2] used a modal method to calculate the scattering from rough surfaces with random rectangular grooves, all of the same depth. They also calculated for finitely conducting materials forming the surface. Mendoza-Suárez and Méndez [3] presented an integral equation method which has also been used to resolve the scattering from rectangular grooved surfaces and for this method the depth, width and separation of the grooves can vary. Also, a reformulation of the Kirchhoff method was recently presented [4,5] which permits the multiple scatter calculation of infinite-slope surfaces; again, this method is applicable to surfaces with variable depth, width and separation of the grooves. Hollins and Jordan [6] measured the intensity distribution and the speckle statistics of a telegraph signal form phase screen. Surfaces with rectangular-shaped grooves can be produced experimentally using ion-beam milling techniques [6] or by optical lithography using photoresist materials [7,8].

The phenomenon of enhanced backscatter has been widely studied in the literature. One of the mechanisms responsible for the effect is the coherent interference of a ray with its time-reversed (the same ray traversed in the opposite direction) partner. When both of these rays are reflected back towards the source, there is no phase difference between them and they add coherently; when they add in other directions, the phase difference is a function of the scatter angle, the wavelength and the separation of the scatter points on the surface. In a surface with rectangular groove surfaces (for a 1D problem, see Fig. 1), the rectangular grooves act like corner cube retro-reflectors, sending the double-scattered rays back in the same direction that they came from (see Fig. 2). In this case, there will always be enhanced backscattering for the double-scattered light due to the double scattering of light within each groove, and there will, therefore, be an enhancement of the retro-reflected light. There is no way of avoiding this effect. However, it is possible to alter the distribution of light within the enhanced backscatter peak using the interference of the light retro-reflected from different grooves. Previously it was shown how the depths of the grooves could be changed to affect the intensity backscattered by the surface [5]. In that work, the interference between the light from different grooves gave an interference pattern superimposed on the enhanced backscatter peak. The interference pattern consisted of a number of intensity peaks which added or subtracted from the enhanced backscatter peak, alternately giving an enhanced backscatter peak with additional points of light or darkness. In this work we show how it is possible, by adding variations of the groove width and separa-

tion, to reduce the side peaks of the interference patterns and control the intensity in the backscatter angle of the enhanced backscatter peak, and leave the remaining scatter angles with almost the same scattered intensity. The resulting designed surfaces are rough in the sense that the correlation functions differ from their mean values only for correlation for a groove with itself; the correlation between different grooves gives the mean value. Numerical scattering patterns are calculated for the designed surfaces using the reformulated Kirchhoff method and the integral equation method.

2. Theory

The reformulated Kirchhoff method [4,5] uses the redefinition of the inward surface normal (see Fig. 1)

$$\mathbf{n} = -\sin \beta \mathbf{x} + \cos \beta \mathbf{y} = -\frac{dy}{dS} \mathbf{x} + \frac{dx}{dS} \mathbf{y} \quad (1)$$

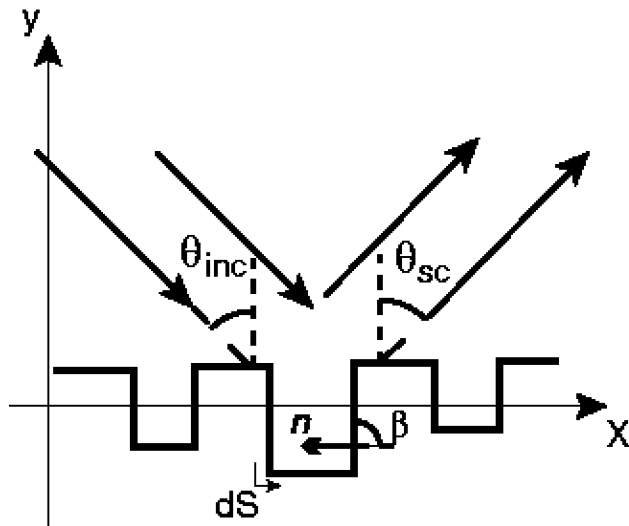


FIGURE 1. The geometry of the problem studied here.

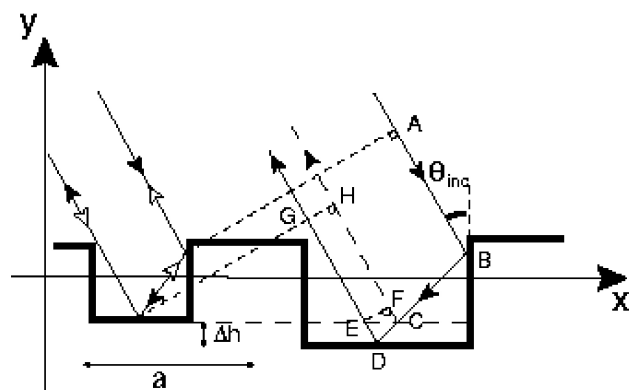


FIGURE 2. The geometry used for calculation of the phase change for double scattered light from two different grooves of different depths. The phase difference is calculated for the rays with the dark arrows. The parameter a is the sum of the groove separation and the groove width.

to give the diffraction equation

$$\begin{aligned} \Phi_{sc} = & \frac{-1}{4\pi} \int S_{inc} S_{sc} \Phi_{inc}(x_s, y_s) \\ & \times \left[(1 + R) \sin \theta_{sc} H_1^{(1)}(kr) \right. \\ & \left. - i(1 - R) \sin \theta_{inc} H_0^{(1)}(kr) \right] dy \\ & - \frac{1}{4\pi} \int S_{inc} S_{sc} \Phi_{inc}(x_s, y_s) \\ & \times \left[(1 + R) \cos \theta_{sc} H_1^{(1)}(kr) \right. \\ & \left. + i(1 - R) \cos \theta_{inc} H_0^{(1)}(kr) \right] dx, \quad (2) \end{aligned}$$

where Φ denotes the electric field, the subscript *inc* refers to the incident field, the subscript *s* refers to the surface, R is the Fresnel reflection coefficient which depends on the surface material and the local angle of incidence on the surface segment of interest, the subscript *sc* refers to the scattered field, \mathbf{k} is the wavevector of the field, $H_0^{(1)}(kr)$ is the zeroth-order Hankel function, which is the Green function for the one-dimensional Helmholtz equation, $H_1^{(1)}(kr)$ is the first-order Hankel function resulting from the normal derivative of the Green function, and S_{inc} and S_{sc} are geometric shadow functions indicating whether the surface point of interest is illuminated or visible from the detector, respectively.

Double-scattered light is taken into account in the Kirchhoff approximation by first calculating the field at a point on the surface which is scattered from all the other points on the surface:

$$\begin{aligned} \Phi_{sc}^{(1)}(x_2, y_2) = & \frac{-1}{4\pi} \int S_{inc} S_{12} \Phi_{inc}(x_s, y_s) \\ & \times \left[(1 + R_1) \sin \theta_{12} H_1^{(1)}(kr_{12}) \right. \\ & \left. - i(1 - R_1) \sin \theta_{inc} H_0^{(1)}(kr_{12}) \right] dy_1 \\ & - \frac{1}{4\pi} \int S_{inc} S_{12}(x_s, y_s) \\ & \times \left[(1 + R_1) \cos \theta_{12} H_1^{(1)}(kr_{12}) \right. \\ & \left. - i(1 - R_1) \cos \theta_{inc} H_0^{(1)}(kr_{12}) \right] dx_1 \quad (3) \end{aligned}$$

where the subscript 1 refers to the first interaction point on the surface and the subscript 2 the second point, and S_{12} is a geometric shadow function indicating whether point 1 is visible from point 2. This field is then used as the incident field, and the corresponding field scattered from all of the second points on the surface can be calculated:

$$\begin{aligned} \Phi_{sc}^{(2)}(x, y) &= \frac{-1}{4\pi} \int S_{sc} \\ &\times \left[\Phi_{sc}^{(1)}(x_2, y_2)(1 + R_2) \sin \theta_{sc} H_1^{(1)}(kr_{sc}) \right. \\ &\quad \left. - (1 - R_2) \frac{d\Phi_{sc}^{(1)}(x_2, y_2)}{dn_2} H_0^{(1)}(kr_{12}) \right] dy_2 \\ &\quad - \frac{1}{4\pi} \int S_{sc} \left[\Phi_{sc}^{(1)}(x_2, y_2)(1 + R_2) \cos \theta_{sc} H_1^{(1)}(kr_{sc}) \right. \\ &\quad \left. - (1 - R_2) \frac{d\Phi_{sc}^{(1)}(x_2, y_2)}{dn_2} H_0^{(1)}(kr_{12}) \right] dx_2. \end{aligned} \tag{4}$$

The term $[d\Phi_{sc}^{(1)}(x_2, y_2)]/dn_2$ is approximated by taking the derivatives of only the Hankel function terms in Eq. (3). Note that for the double-scatter term the points 1 and 2 cannot coincide, thus there is no problem with the singularities of the Hankel functions.

The integral equation method [3] for scattering of s-polarised light from a perfectly conducting rough surface is given by

$$\begin{aligned} \Phi_{inc}(x, y) - \frac{1}{4\pi} \int H_0^{(1)}(kr) \frac{\partial \Phi(x_s, y_s)}{\partial n} ds \\ = \begin{cases} \Phi(x, y) & \text{if } (x, y) \text{ is above the surface} \\ 0 & \text{if } (x, y) \text{ is below the surface,} \end{cases} \end{aligned} \tag{5}$$

where ds is a surface segment length.

In the calculations presented here, TM (p) polarization was used. It was found that the differences between the results for TE and TM polarization were not detectable in the scattered intensity distributions. In the Kirchoff method, a perfectly conducting surface with TM polarization requires a Fresnel reflection coefficient of -1.

Rectangular shaped grooves contain right angles which act to return the light in the incident direction, back towards the source. As in Gaussian randomly rough surfaces, a backscattered ray and its time-reversed partner (see Fig. 2) will be in phase and will add coherently. This is the enhanced backscatter effect. The phase difference between the backscattered rays coming from different grooves is given by

$$\begin{aligned} \Delta\phi &= k(\text{AB} + \text{CD} + \text{DE} + \text{EG}) \\ &= k(\text{AB} + \text{CD} + \text{DE} + \text{CH} - \text{CF}), \end{aligned}$$

where $k = 2\pi/\lambda$ and

$$\begin{aligned} \text{AB} &= \text{CH} = a \sin(\theta_{inc}) \\ \text{CD} &= \text{DE} = \frac{\Delta h}{\cos(\theta_{inc})} \\ \text{CF} &= 2\Delta h \tan(\theta_{inc}) \sin(\theta_{inc}). \end{aligned}$$

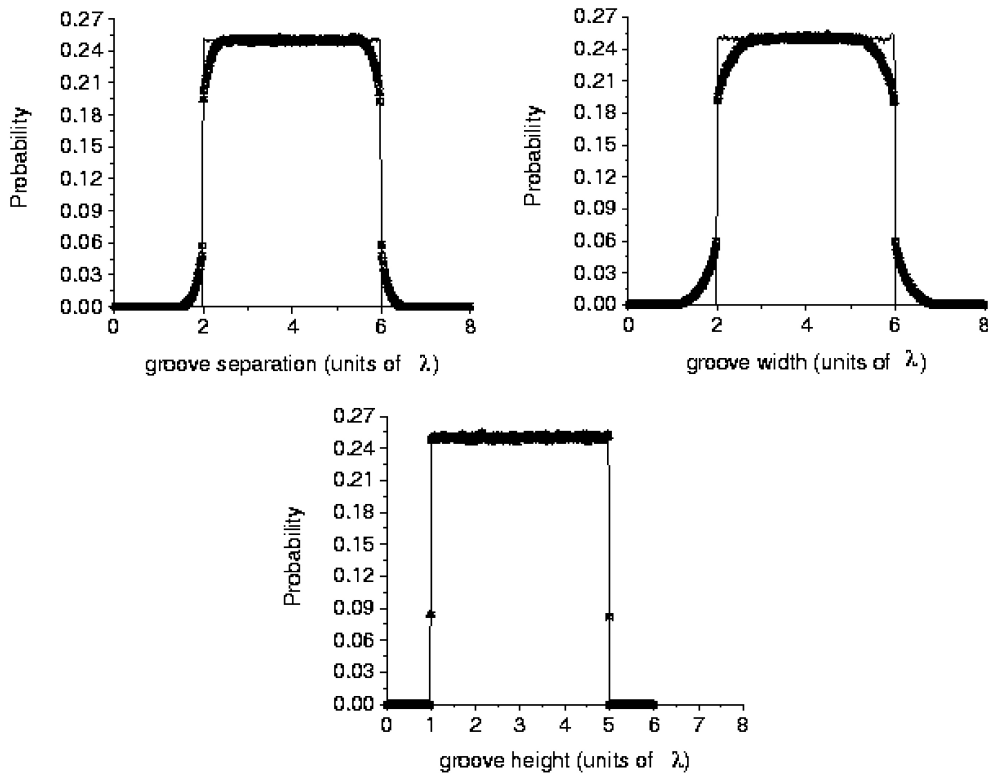


FIGURE 3. Probability distributions for the groove width (top left), groove separation (top right) and groove height (bottom) for 40000 realizations of a surface with 20 grooves. Full line, random distribution; open circles, adjusted surface with equation (9) and $\Delta\varphi = (m + 0) 2\pi$; crosses, $\Delta\varphi = (m + 0.25) 2\pi$; and open triangles, $\Delta\varphi = (m + 0.5) 2\pi$. In this case the groove heights were not changed. Note that the probability distributions of the adjusted surfaces are independent of the phase difference used in the surface design.

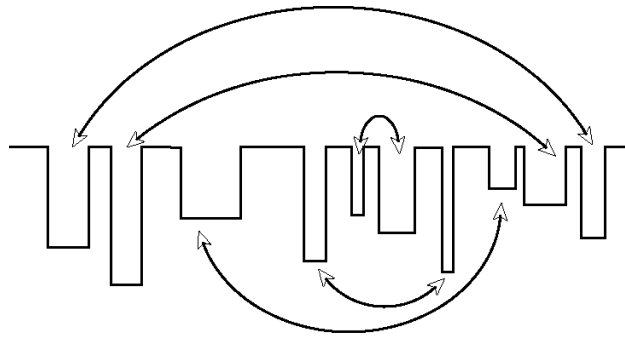


FIGURE 4. The arrangement of the pairs of grooves used for the surface design. The pair of grooves in the centre of the surface are adjusted first and then the successive pairs of grooves nearest the centre until the outermost pair is adjusted.

The phase difference is then

$$\Delta\phi = 2k \left[a \sin(\theta_{inc}) + \Delta h \left(\frac{1}{\cos \theta_{inc}} - \frac{\sin^2 \theta_{inc}}{\cos \theta_{inc}} \right) \right]$$

$$= 2k [a \sin(\theta_{inc}) + \Delta h \cos \theta_{inc}], \tag{6}$$

i.e. the phase difference depends on the separation of the two grooves a (which depends on the width and separation of the grooves) and the difference in the depth of the two grooves

Δh , as well as on the incidence angle and the wavelength. The purpose of this paper is to show how Eq. (6) can be used to design randomly rough surfaces with infinite slopes with specific scattered intensities in the backscattered direction.

The intensity in the backscattered direction depends on the interference term: for $\Delta\phi = (m + 0)2\pi$ there will be constructive interference, and for $\Delta\phi = (m + 0.5)2\pi$ there will be destructive interference.

3. Surface generation

For a surface with many grooves, we require that the grooves can be grouped together in pairs for which the separations and depths satisfy Eq. (6) with the required value of the phase difference. The rough surfaces are generated by first generating the groove widths, the groove separations and the groove depths or heights from independent probability distributions with predefined average values and widths of the rectangular probability distributions (see Fig. 3). Then the grooves are taken in pairs, starting from the two central grooves and the widths, separations and heights of the grooves are adjusted to satisfy Eq. (6). Once the two central grooves are fixed to satisfy Eq. (6) the next two grooves (the next to the left and the next to the right of the two central grooves (see Fig. 4) are

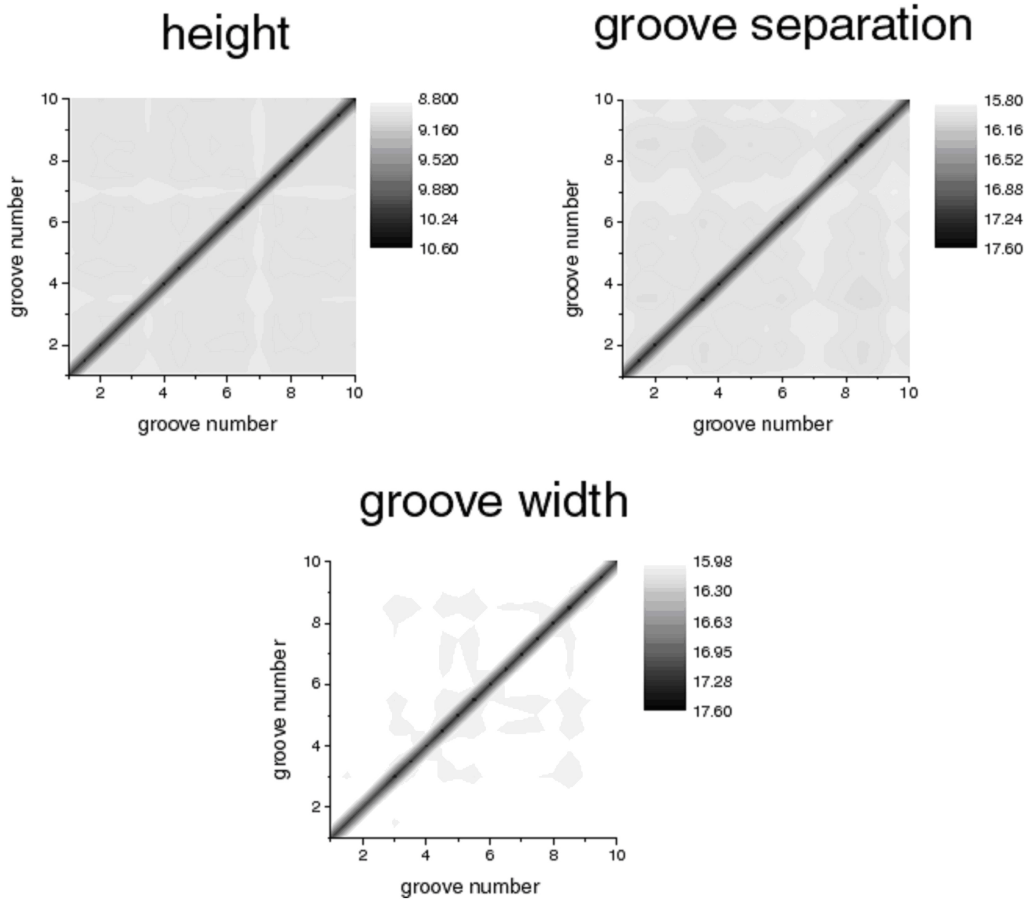


FIGURE 5. Correlation functions $\langle h_i h_j \rangle$, $\langle d_i d_j \rangle$ and $\langle c_i c_j \rangle$ for 40000 realizations of a surface with 20 grooves. It can be seen that there is no correlation between different grooves.

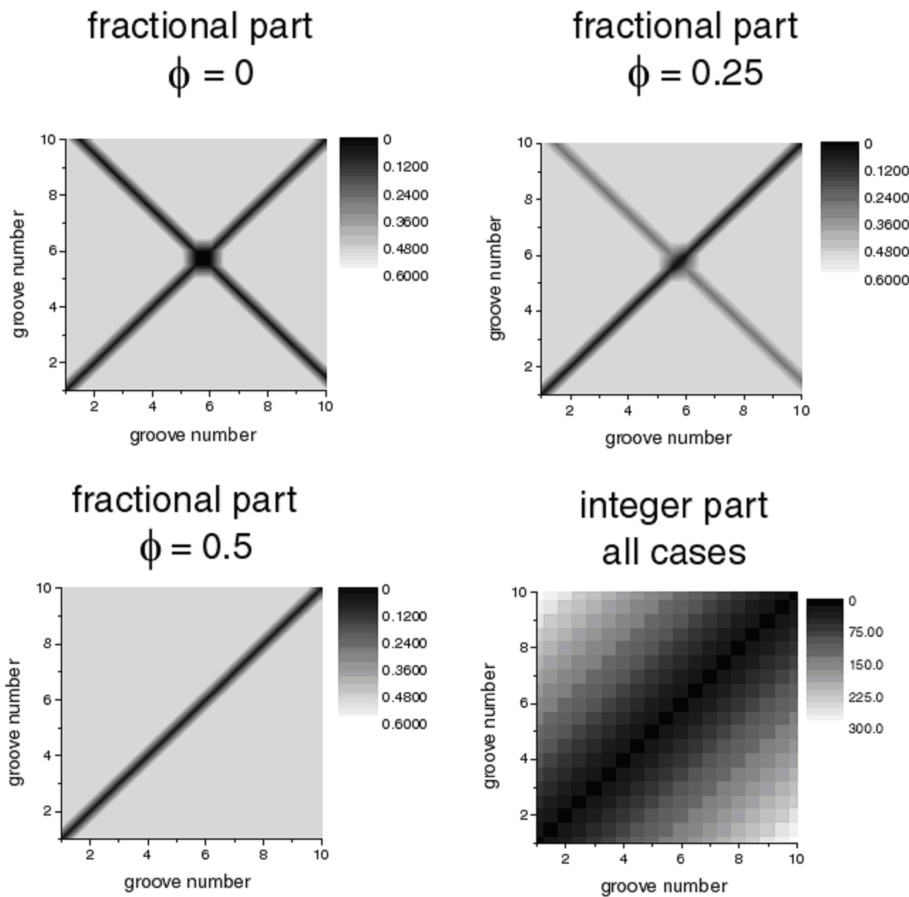


FIGURE 6. Graphs of the correlation function $\langle 2k (a \sin(\theta_{\text{inc}}) + \Delta h \cos \theta_{\text{inc}}) \rangle$. The fractional parts show the relation between the grooves used in the surface design in the diagonal from top left to bottom right. The integer part is the same for all cases and increases for larger groove separations.

adjusted, and so on until all the grooves are arranged to give the correct phase difference. The adjustments in the widths, separations and heights or depths are made in such a way that the probability distributions of these parameters are symmetrical (see Fig. 3) with the same mean as the original random distribution. We define the correlation function

$$\langle x_i x_j \rangle = \sum_N x_{iN} x_{jN}$$

with x_{iN} being the value of the variable x for the i 'th groove of the N 'th realization of the random surface. A total of 40000 realizations of the surface (different combinations of the random parameters used but with the same probability distributions) were used to calculate the correlation functions. The resulting surfaces are random in the sense that the correlation functions $\langle h_i h_j \rangle$, $\langle d_i d_j \rangle$ and $\langle c_i c_j \rangle$ show no correlation between the grooves i and j (Fig. 5, note that, since the depth, separation and width of the grooves do not have zero mean, the background values of the correlations are not zero, but rather are given by the square of the mean values). However, graphing the function $\langle 2k[a \sin(\theta_{\text{inc}}) + \Delta h \cos \theta_{\text{inc}}] \rangle$ (Fig. 6) shows the relation between the pairs of grooves used in the surface design. Finally, Fig. 7 shows two examples of the surface shapes for the two cases studied here. The variations

of the surface profile for different phase differences (between 0 and 0.5λ) in the surface design are too small to be seen clearly on these graphs.

4. Results

All the results presented here are for a perfectly conducting surface material and a 1D rough surface with plane wave illumination. The surfaces were divided into 4000 points for the numerical calculation and the final results were averaged over 200 realizations of the random surface with the same statistics. The calculation took approximately 5 minutes per realization on a 2.4 GHz PC. For all cases, the normalized (with respect to the incident energy) integrated scattered energy from the rough surfaces was between 0.97 and 1.03, *i.e.* with an error of $\pm 3\%$ (the normalized integrated scattered energy should be 1 for a perfectly conducting surface). Figure 8 shows an example of the results obtained with the new Kirchhoff method and the surfaces designed as described above. This figure shows the single scatter (black curve), double scatter (gray curve) and total (sum of single and double scatter) (black crosses) for a surface with 8 lines above the plane reference surface, an average line separation of 4λ and a

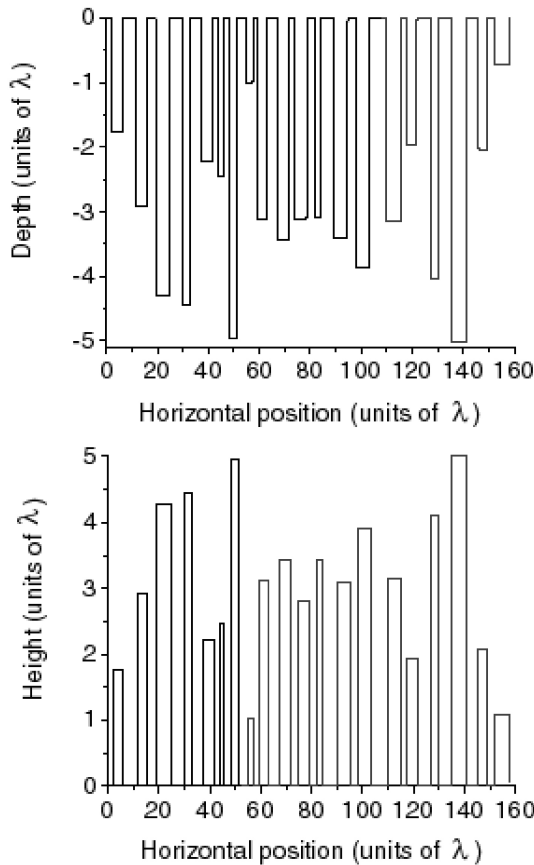


FIGURE 7. Examples of the surfaces generated for grooves (top) and lines above the surface (bottom). The curves are for $\Delta\phi = (m + 0)2\pi$.

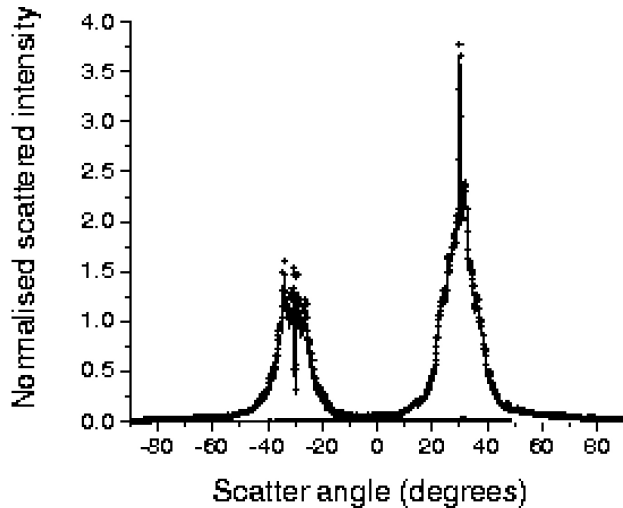


FIGURE 8. Graph showing the single scatter (black curve), double scatter (gray curve) and total (sum of single and double scatter) (black crosses) for a surface with 8 lines above the plane reference surface, an average line separation of 4λ and a variation of $\pm 2\lambda$, an average line width of 4λ and a variation of $\pm 2\lambda$, and an average line height of 3λ and a variation of $\pm 2\lambda$. The line height was not adjusted in the designed surface, and the designed phase difference was $\Delta\phi = (m + 0.5)2\pi$. The designed incidence angle was 30° .

variation of $\pm 2\lambda$, an average line width of 4λ and a variation of $\pm 2\lambda$, and an average line height of 3λ and a

variation of $\pm 2\lambda$. The line height was not adjusted in the designed surface, and the designed phase difference was $\Delta\phi = (m + 0.5)2\pi$. The designed incidence angle was 30° . It can be seen that, as expected, the single scatter contribution appears in the specular direction and the double-scatter term in the backscatter direction. The double-scatter peak corresponds to the enhanced backscatter peak in these cases because all of the double scattered rays are directed back towards the source. In the double scatter term it can be seen that there is a narrow ($< 0.4^\circ$ wide limited by the resolution of the calculations) minimum in the backscatter direction, as is expected for the case of $\Delta\phi = (m + 0.5)2\pi$. Note that the width of the interference peak in the backscatter direction depends on the widest separation of the grooves contributing to the interference. A different arrangement of the pairs of grooves will give a different width of the interference peak.

Figure 9 shows only the double scatter case for the same surface as Fig. 8, but with different phase variations used for the surface design. The phase differences are: $\Delta\phi = \text{random}$, top left; $\Delta\phi = (m + 0)2\pi$, top right; $\Delta\phi = (m + 0.5)2\pi$, bottom left; and $\Delta\phi = (m + 0.25)2\pi$, bottom right. For all these cases, the single scatter term was indistinguishable on the same scale. It can be seen that for the random surface the double-scatter term is smooth with no structure in the backscatter direction. However, the intensity in the backscatter direction depends on the phase difference used in the surface design. For $\Delta\phi = (m + 0)2\pi$, there is an interference maximum in the backscattered direction; for $\Delta\phi = (m + 0.5)2\pi$, there is a minimum; and for $\Delta\phi = (m + 0.25)2\pi$, there is a point of inflexion, with a small maximum at smaller negative scatter angles and a small minimum for larger negative scatter angles, as expected from the interference model used in the surface design. It can also be seen that there are still secondary interference peaks at -34° and -26° . These peaks correspond to the position where the contributions from the pairs of grooves have a phase difference π different from the phase difference in the backscatter direction. This can be calculated from Eq. (6), assuming that the phase difference from (6) is given by

$$\Delta\phi = 2k(a \sin(\theta_{inc}) + \Delta h \cos \theta_{inc}) = (m + 0.5)2\pi. \quad (7)$$

Then, writing the equation for the phase difference for different incidence and scatter angles, and requiring that this phase difference be π different from the value in Eq. (7) gives

$$k[a \sin(\theta_{inc}) + \Delta h \cos \theta_{inc}] + k[a \sin(\theta) + \Delta h \cos \theta] = \begin{cases} (m + 0)2\pi \\ (m + 1)2\pi, \end{cases} \quad (8)$$

where θ is the scatter angle. Substituting (7) into (8) and rearranging terms gives

$$2k[a \sin(\theta) + \Delta h \cos \theta] = \begin{cases} (m - 0.5)2\pi \\ (m + 0.5)2\pi. \end{cases} \quad (9)$$

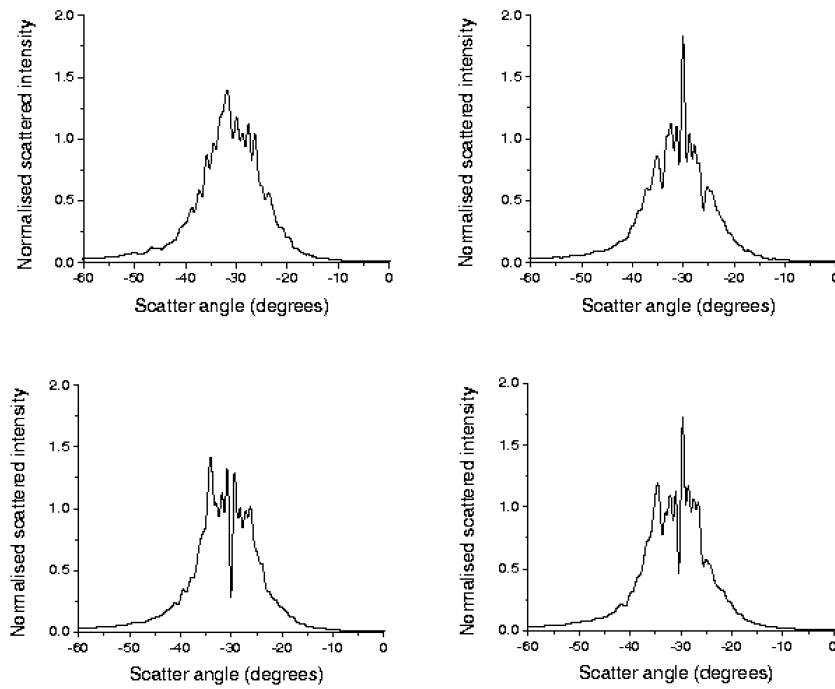


FIGURE 9. Graphs of the double scatter contributions for the same surface as figure 8 but with phase differences of: $\Delta\phi = \text{random}$, top left; $\Delta\phi = (m + 0) 2\pi$, top right; $\Delta\phi = (m + 0.5) 2\pi$, bottom left; and $\Delta\phi = (m + 0.25) 2\pi$, bottom right. For all these cases the single scatter term was indistinguishable on the same scale.

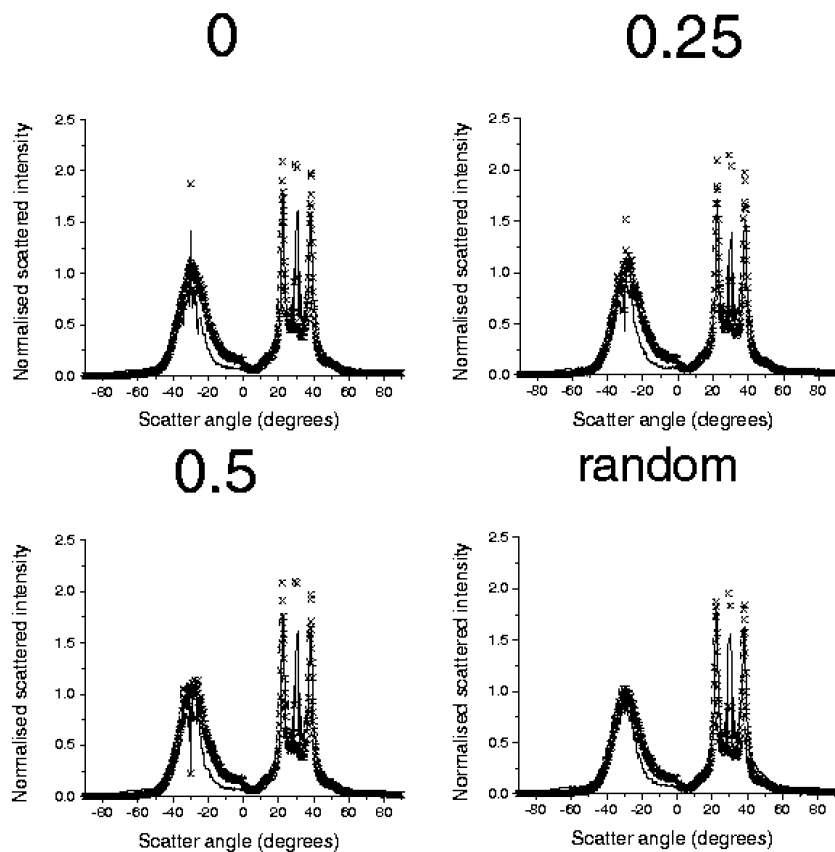


FIGURE 10. The light scattered from a random surface of grooves in a flat plane. The value of the designed phase difference is shown above each graph. The continuous lines are the results of the calculation with the integral equation method and the crosses are the results of the modified Kirchhoff method. The surface figures are as given in Fig. 8 and the incident angle is 30° . The surfaces contained 8 grooves.

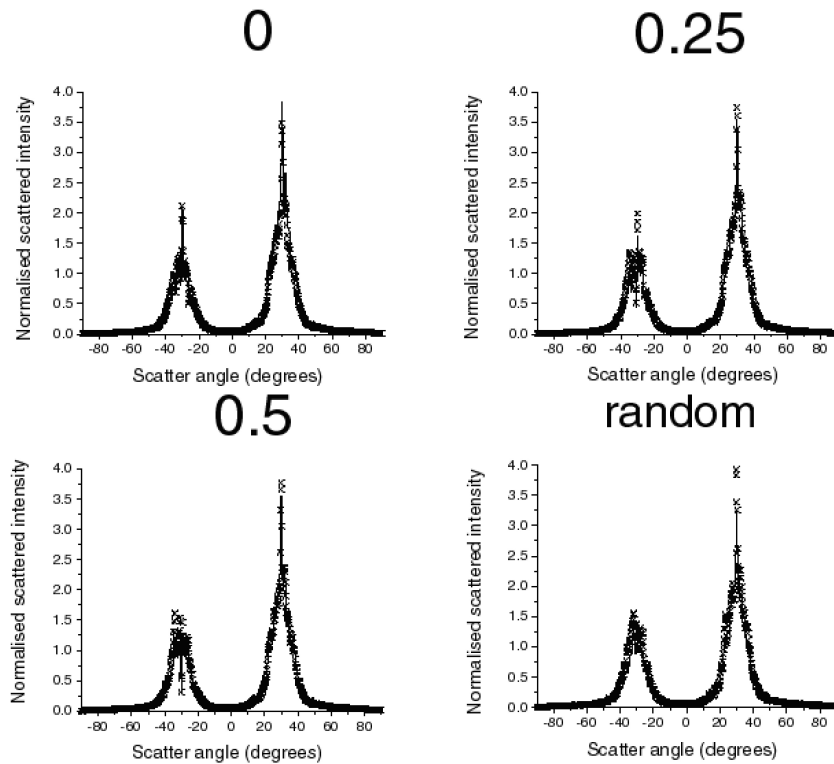


FIGURE 11. As Fig. 10 but for a random surface with lines above the flat plane.

Eliminating m from (8) and (9),

$$2k\{a[\sin(\theta_{\text{inc}}) - \sin(\theta)] + \Delta h(\cos \theta_{\text{inc}} - \cos \theta)\} = \begin{cases} 2\pi \\ -2\pi. \end{cases} \quad (10)$$

To estimate the value of θ from Eq. (10) we take the average values of the terms a and Δh over the surface:

$$2k\{\langle a \rangle[\sin(\theta_{\text{inc}}) - \sin(\theta)] + \langle \Delta h \rangle(\cos \theta_{\text{inc}} - \cos \theta)\} = \begin{cases} 2\pi \\ -2\pi. \end{cases} \quad (11)$$

From the parameters given above for the rough surfaces $\langle a \rangle = 8\lambda$ and $\langle \Delta h \rangle = 0$, we have

$$\sin(\theta_{\text{inc}}) - \sin(\theta) = \pm \frac{\lambda}{2\langle a \rangle} \quad (12)$$

and with $\theta_{\text{inc}} = 30^\circ$, $\theta = 34.22^\circ, 25.94^\circ$, in very good agreement with the results of the calculations.

Figures 10 and 11 show the comparison between the modified Kirchhoff method presented here and the integral equation method presented in Ref. 3 for the surfaces presented above. In Fig. 10 the results are for the light scattered from a random surface of grooves in a flat plane. The value of the designed phase difference is shown above each graph. The continuous lines are the results of the calculation with the integral equation method, and the crosses are the results of the modified Kirchhoff method. The surface figures are as given in Fig. 8 and the incident angle is 30° . The surfaces contained 8 grooves. Figure 11 shows the same as Fig. 10 but

for lines above a flat plane. It can be seen that the agreement between the results of the two methods is very good. The Kirchhoff method tends to slightly overestimate the energy in the double-scatter contribution, particularly with grooves in a flat plane, perhaps due to the limitations of the geometrical shadow functions used in the calculation (these shadow functions do not take into account the diffraction at the surface edges). The variation of the backscattered intensity with the designed phase difference can be seen to be as expected in all cases.

5. Conclusions

In this paper, it has been shown that the backscattered intensity from a random rectangular-grooved surface can be controlled with small (fractions of a wavelength) changes in the roughness parameters. Numerical calculations performed with a modified Kirchhoff method and with the integral equation method show good agreement and confirm the intensity variations. Note that the effect presented here is an interference effect so that it is wavelength dependent. The intensity required in the design can only be achieved at the designed wavelength.

Acknowledgements

This work was partially supported through project IN101502 from DGAPA, UNAM.

1. E. Jakeman and B.J. Hoenders, *Optica Acta* **29** (1982) 1587.
2. R.A. Depine and D.C. Skigin, *J. Opt. Soc. Am. A* **11** (1994) 2844.
3. A. Mendoza-Suárez and E. R. Méndez *Applied Optics* **36** (1997) 3521.
4. N.C. Bruce, *Applied Optics* **42** (2003) 2398.
5. N.C. Bruce, *Applied Optics* **44** (2005) 784.
6. R.C. Hollins and D.L. Jordan, *Optica Acta* **30** (1983) 1725.
7. P.F. Gray, *Optica Acta* **25** (1978) 765.
8. E.R. Méndez and K.A. O'Donnell, *J. Opt. Soc. Am. A* **4** (1987) 1194.